Original Research Article

Rainfall distribution in the Brazilian Amazon: application of the variogram function to time series

.

ABSTRACT

The Amazon area is vast and diversified, with several climatic zones that influence directly in the associated ecosystems. This research analyzed the annual (hydrological year) and seasonal (drought and wet) climatological patterns of the Brazilian Amazon (North Region) between 1991–2022. The incomplete Gamma distribution model, kriging and cokriging interpolation tests, estimates of mean precipitation by the isohyet method, and of precipitated volume by the contour method were applied to numerical data. Data normalization techniques and image interpolation also contributed to identify precipitation patterns and trends in the northern region of Brazil. The method of hierarchical grouping by minimum variance was used, aided by the construction of frequency histograms and tests of significance. The results indicated a strong seasonality of rainfall. The highest precipitation rates occurred in the N-NW axis and the lowest in the south equatorial zone. The active atmospheric systems played an important role in the distribution of rainfall, both annual and seasonal. Four distinct climatic zones were established: southern, central, northwestern and northeastern. Based on the frequency of rainfall determined at levels of 10 to 90% probability, the results suggested a trend in the number of days with precipitation between 25 and 50% in most of the southern and central zones and an increase in precipitation from 50 to 75 % in the northern region. The ordinary kriging test and the spherical semivariogram model showed the best results for data interpolation, with better responses to the behavior of climatic variables and solutions for the spatial-temporal discontinuity of historical series. The results indicated a tendency towards the presence of isotropic climatic phenomena, especially in the wind distribution model. The results showed that they could support the understanding of the distribution of rainfall in the Amazon region.

Keywords: *Hyetogram; Gamma distribution; Kriging; Cokriging; Functional shutdown*

1. INTRODUCTION

The climate of a region is the result of the interaction of several factors at different geographic scales. On a large scale, the circulation of global air masses is related to the movement of ocean currents. On the regional scale, geographic aspects such as relief, altitude and latitude stand out; these are associated with the typology of biomes. This is a relationship strongly influenced not only by geographic aspects, but also by the use and occupation of the land.

The Amazon plays an important role in controlling and balancing the global atmospheric circulation and hydrological cycle. This happens as a result of its immense territorial dimension, associated with water dynamics and availability, and its location within the equatorial zone, which has a high incidence of solar radiation and precipitation. In Equatorial zone, rainfall is among the most important and influential meteorological elements in environmental conditions, controlling the regional water balance. Several studies have attested to this specifically for the Amazon region [1-7]. Through the continuous study of precipitation at different scales (daily, seasonal, annual, decennial) it is possible to establish periods of greater or lesser rainfall [8]. Such considerations not only allow a better

understanding of climatic aspects (hydrological cycle) and the oscillation of the river-lacustrine system (seasonal water cycle), but also provide subsidies for the establishment of management plans aimed at agriculture and urbanization.

Despite being relevant, analyzing the precipitation pattern in a region as vast and complex as the Amazon is still a challenge, mainly due to the high space-time variation of regional rainfall. The application of historical series in the study of the Amazonian climate has been increasingly effective, especially because of global climate changes associated with local deforestation. In this sense, works of [9-12] are included.

The northern region of Brazil encompasses most of the Brazilian Amazon. Despite its importance in the global climate context, the study of time series in the region still faces difficulties with insufficient or discontinuous data collection. There are several geographic spaces with an absence of information due to the lack or deactivation of climatological stations. To compensate for this space-time deficiency in the measurement data, statistical techniques are applied, which include similarity analysis, linear regression, and data normalization techniques with the application of weighted averages, in addition to probabilistic models and the use of image interpolation from cartographic bases. Rainfall distribution models have been increasingly applied in ecological studies, as precipitation directly interferes with the balance of ecosystems, in the production of organic matter, in plant and animal physiology, and in the regional hydrological regime. The objective of this study was to analyze the spatial-temporal distribution of the rainfall, identifying its annual and seasonal pattern in the North region of Brazil, using geostatistics associated with historical series (1991–2022).

1.1 Climate Aspects of the Region

The Brazilian Amazon, with an area greater than five million km^2, represents about 58.9% of the national territory, and covers parts of nine states, seven of which are located in the North geographic region of the country (Fig. 1), which, in turn, represents 45.2% of the Brazilian territory. The large water network inserted in this complex mosaic of ecosystems plays an important role in the exchange of energy and humidity for the water-earth-atmosphere system, whose result is the maintenance and regulation of the climate from the local to the global level. The distribution of rainfall in the North is related to the dynamics of important atmospheric systems. The Continental Equatorial Air Mass (mEc) is centered in the west of the region, between Brazil, Colombia and Venezuela. It is characterized by strong humidity, resulting from the processes of evaporation and evapotranspiration of the Amazon biome, with contributions from moist air masses from the Atlantic Ocean. The Intertropical Convergence Zone (ITCZ) is formed by the convergence of the NE and SE trade winds. The ITCZ plays an important role in producing rain in coastal areas, including eastern Pará and the mouth of the Amazon River. The Tropical Instability Line (TIL) is characterized by the accumulation of aligned clouds formed by the circulation of the sea breeze and high incident solar radiation, especially active in the states of Amapá and Pará. The General Circulation of the Alta Bolivian (AB) is an anticyclone active in the high troposphere during the summer months, starting from the Andean region towards the coast. Cold fronts come from extra-tropical latitudes and often reach the southern limit of the states of Rondônia, Amazonas and Pará. They are responsible for the phenomenon regionally called '*friagem*', with the formation of frontal rains over the southern part of the Amazon during the dry season. Also influencing the precipitation rate are meteorological phenomena on a global scale: El Niño – Southern Oscillation (ENSO), a large-scale phenomenon originating in the tropical Pacific Ocean and associated with atmospheric changes, and the Atlantic Dipole [1-4,6,13].

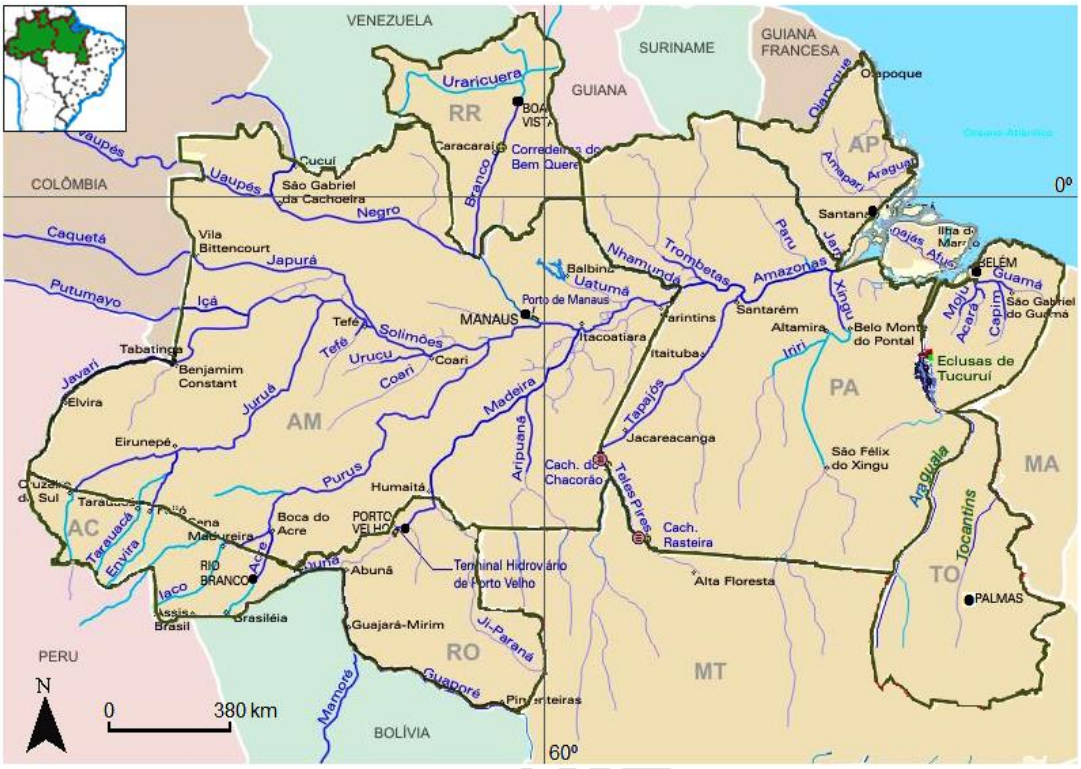

Fig. 1. River basin chart of the North Region of Brazil. (Source: IBGE - Atlas Geográfico Escolar, 2016 modify).

The result of the joint action of these atmospheric systems in the Amazon is the predominance of a hot and humid Equatorial (*Af*) climate, with a high precipitation rate and low annual variation. There is still a strong influence of the monsoon climate (*Am*) to the east, with hot and humid air masses coming from the ocean, with significant participation of the humid forest; and a drier savanna climate (*Aw*) in the S–SE of the states of Amazonas and Pará, influenced by the Cerrado biome, as well as in the northeast of Roraima, where the dry climate tends to last between December and March, establishing an 'area drought' due to little interference from the mEc and ITCZ circulation systems. According to the survey of geodiversity prepared by SGB/CPRM [14], this amplitude oscillates between 1800 and 3100 mm/year, with an average for the central region of 2200±200 mm/year. From this extensive variation, it is possible to identify at least five different rainfall regimes: the first located on the W–NW axis close to the Pre-Andean region, with greater rainfall between April and June; the second in the far north of the states of Amazonas and Roraima, with the rainy season concentrated between June and August, and the dry season between December and February; the third in the Central Amazon region, with greater precipitation between March and May and severe drought between June and August; the fourth rainfall regime is located on the NE–E axis, between the coast of Amapá and Pará (Eastern Amazon), with greater precipitation between February and April and a dry period between August and October; and the fifth in the southern limit of the Amazon with rains concentrated between December and February [1,4,15].

2. METHODOLOGICAL PROCEDURES

Climatological data from the seven states located in the North of Brazil were analyzed, totaling 393 monitoring stations in 95 municipalities (Fig. 2). The results referring to the stations inserted in the river basin of the Solimões-Amazonas System were evidenced, with the purpose of, in a second moment, correlating the rainfall model with the water cycle (flood and ebb) in the respective river-lacustrine system. For the period between 1991 and 2022, primary and secondary data were analyzed. Secondary data (historical series) were consulted through hydro-meteorological networks and database managed by the National Water Agency [16,17]; Brazilian Institute of Geography and Statistics [18]; National Institute for Space Research – Center for Weather Forecast and Climate Studies [19]; Meteorological Database for Teaching and Research of the National Institute of Meteorology [20]; Geological Service of Brazil (SGB/CPRM) [14], and National Department of Transport Infrastructure [21], which have stations and/or monitoring programs in the municipalities and basins in the area covered by the study. The location of the set of weather stations consulted is shown in Figure 2. Historical data were tabulated, and their consistency verified by computational software CLIMA [22], developed by the Agronomic Institute of Paraná – IAPAR. Daily data were checked and organized by month, year and seasonal period (drought and rain), to be later grouped into classes.

Quantitative and qualitative analysis of precipitation (mm), including volume, intensity and space-time distribution; of wind (m/s) with direction and maximum gust; relative air humidity (%); atmospheric pressure (mb); global radiation (kJ/m²); and air and dew temperature (ºC) were measured and/or acquired for the region studied. The results were compiled into measures of position and dispersion and analyzed in probabilistic terms by applying a theoretical distribution model adjusted to the data series. Considering precipitation as a continuous random variable, the determination of different levels of probability (25, 50 and 90%) was obtained through the incomplete Gamma distribution model [23], whose density function *F(x)* derives from equation 1, with the respective adjustments to obtain the symbols of the gamma function *f(x)* (Γ; eq. 2). The estimation of α parameter of the Gamma distribution comes from the maximum likelihood method, originally proposed in equation 3. Based on the method of moments, which consists of matching the mean ($\overline{X}$) and variance (S^2) of the sample to the respective measurements in the population, as suggested by [24], α and β parameters were obtained from equations 4 and 5.

$$F(x) = \frac{1}{\beta^{\alpha}\Gamma(\alpha)} x^{\alpha-1} e^{-x/\beta} \quad (1)$$

$$\Gamma(\alpha+1) = \sqrt{2\pi\alpha}\ \alpha^{\alpha} e^{\alpha} \left(1 + \frac{1}{12\alpha} + \frac{1}{288\alpha^2} - \frac{139}{51840\alpha^3}\right) \quad (2)$$

$$\alpha = \frac{1 + \sqrt{1 + \frac{4(\ln \overline{X} - \overline{X_g})}{3}}}{4(\ln \overline{X} - \overline{X_g})} \quad (3)$$

$$\alpha = \frac{\overline{X^2}}{S^2} \quad (4) \qquad \beta = \frac{S^2}{\overline{X}} \text{ or } \beta = \frac{\overline{X}}{\alpha} \quad (5)$$

Where: *F(x)* is the probability of a value ≤ x occurring; α is the shape parameter (dimensionless); β is the scale parameter (mm); *x* is the random variable, equivalent to the monthly or seasonal precipitation (mm) and established as 0< x <∞; Γ is the gamma function [*f(x)*] of parameter α, defined according to

equation 2; $\overline{X}$ is the arithmetic mean and $\overline{X_S}$ is the geometric mean of precipitation (mm); and S^2 is the Variance (mm^2). Still having as condition of existence α and β >0, and *f(x)*= 0 for x <0.

In order to confirm the tendency presented in the precipitation model, the Kolmogorov-Smirnov test was applied with 5% of significance, based on the module of the greatest difference between observed and estimated probability, considering the number of observations in the series under test. For the best fit, both the model and the statistical test were applied to the climatological variables. Considering that the classification variables are measured in different units, the technique suggested by [25], whose values are previously standardized, was adopted to have a zero mean and unitary variance. Several hierarchical clustering techniques have been proposed, such as single linkage, complete linkage, centroid, median, group average and Ward's method. In this study, the method of minimum variance was chosen [26]. The results of the analysis were presented within the concept of geographical climatology through interpolated images of precipitation, temperature, and relative humidity and tested by the methods of kriging and cokriging. The ordinary kriging model was applied to the data, selecting the respective altitudes of each station or monitoring point through the Shuttle Radar Topography Mission (SRTM) elevation raster to give partial heterotopic to the data set. The maps with kriging interpolation were prepared from cartographic bases made available by IBGE, ArcGIS Web Application – ©2022 and NASA SRTM raster, using the UTM projection (zone 20 north) and Datum Sirgas 2000, with numerical scales of 1:250,000 and 1:500,000. The final maps were created using the software ArcMap® 9.3 ©2008 and Surfer® 9.11.947 ©2010 Golden Software, Inc. The semivariogram was used as a basic tool to quantitatively analyze the variation of regional climatic events. In this study, it was decided to adopt the spherical and Gaussian semivariogram models, in order to observe whether the phenomena are isotropic (do not change with the direction) or anisotropic (the variogram function changes with the direction). Thus, the covariance was calculated according to [27] in four horizontal directions: 0°, 45°, 90° and 135°.

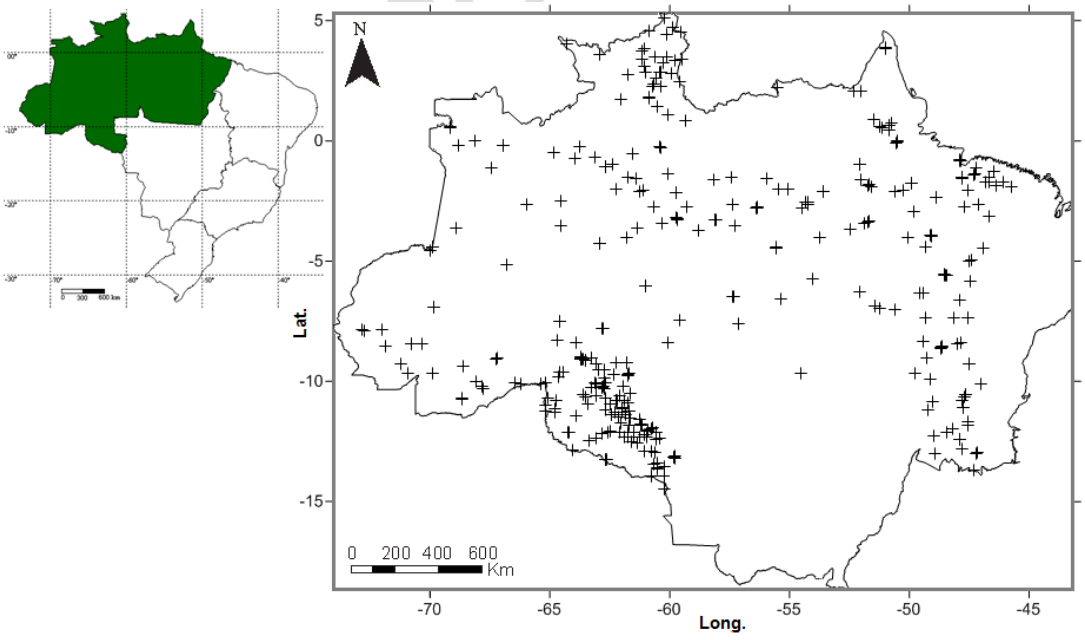

Fig. 2. Distribution of conventional and automatic meteorological stations consulted for the application of the rainfall model in the Amazon – North Region of Brazil (Legal Amazonian Map generated in ArcGis® 9.3 ©2008).

3 RESULTS AND DISCUSSION

3.1 Monthly analysis by capitals

Table 1 presents a summary of climatological data for the seven state capitals in the northern region of Brazil. The average data compiled in the table are representative of the daily punctual data analyzed (month by month) between 1991 and 2022. In general, the results confirm the patterns of regional seasonality, with different periods of drought and rain, confirmed by the correlation of precipitation with the relative humidity of the air (RH). The municipalities located in the southern part of the Brazilian Amazon, exemplified by the cities of Rio Branco in Acre, Porto Velho in Rondônia and Palmas in Tocantins, showed a pattern of drought centered between the months of June and September, with average rainfall for the period of 11.7 in Palmas to 36.9 mm/month in Porto Velho. Manaus (AM), in the Central Amazon, had a similar rainfall pattern, with a dry period centered between the months of July and September but with a higher average precipitation for the period of 60.1 mm/month. The northern climatic zone, on the other hand, presented divergent patterns between the east and west regions. On the east side, the municipalities of Belém (PA) and Macapá (AP), under the greater influence of humid air masses originating from the ocean, highlighting the Intertropical Convergence Zone (ITCZ) and the Tropical Instability Line (TIL), had the period drought defined for the months of July to November in Belém, with an average of 110.3 mm/month; and between August and October in Macapá, with an average of 52.9 mm/month. Historically, the relative humidity of the air in these two capitals has never been below 69%, suggesting that there is an attenuation of the drought due to the entrance of oceanic moisture masses throughout the entire annual hydrological cycle. On the western axis of the northern climatic zone, the municipality of Boa Vista (RR) had a longer dry period, ranging from five to six months (November to March), coinciding with summer in the Southern Hemisphere. At that point, the average for the dry season was 29.4 mm/month. Boa Vista is under the influence of high troposphere anticyclones, which during the hot months displace dry air masses from the Andean and Pre-Andean regions towards the coast, directly interfering with the volume of precipitation in the region. Although the divergences were found on the E-W axis, the drought was much milder compared to the patterns observed in the central and southern climate zones. It should be noted that years of significant oscillation were observed in the patterns of distribution and intensity of rainfall in the aforementioned regions, especially due to the influence of global teleconextion meteorological phenomena such as El Niño and La Niña. Despite this, rainfall distribution trends followed regional seasonal patterns. The incident solar radiation varied greatly over the period, oscillating between 470 and 23,045 kJ/m^2 (average 2016 kJ/m^2), largely due to the variation in the measurement time and the constant presence of clouds, especially between the southern and northeastern climatic zones, which significantly reduced the albedo. However, large variations in air temperature were not observed in the period measured for the entire northern region, which ranged in average values between 25 and 28 ºC (26.9±1.3 ºC).

3.2 Monthly analysis by climate zones

Among the meteorological elements, rainfall is the element that most influences environmental conditions in the tropics, with a direct effect on the water balance (water – atmosphere – soil system) and acting on other elements such as temperature, air humidity and solar radiation [8,28,29]. Precipitation has a preponderant action on the hydrological

conditions, interfering with the flood and ebb patterns in the hydrographic basins. From the continuous quantitative data of precipitation for the North region of Brazil, in the period between January 1991 and December 2022, it was possible to analyze the distribution of rainfall frequency for the monthly and seasonal data (drought and rain) for each sub-region.

The number of classes (*k*) of the frequency distribution was determined based on two criteria: the Sturges rule, which establishes a *k* from the logarithm of the sample number (*n*); and in the literary consensus, which recommends, whenever possible, a number of classes between 5 and 20 [30], depending on the amount of data available. The argument is that some classes may result in little information being extracted from the table. On the other hand, a high number of classes tend to construct classes with zero or very little frequency, resulting in an irregular distribution of results. Thus, the number of nine classes was established for all the studied climate zones (Table 2), considering the sample number between 1209 (AP) and 5609 (TO). It was not possible to relate the absolute frequency distribution (*f*) of monthly rainfall averages with an average rainfall pattern for the study area. This is due to the large variation in values in each sub-region. Since it is not feasible to establish a total probability of precipitation, we tried to analyze the results by climate zone.

Table 1. Summarized climatological data from 1991 – 2022 for the seven capitals of the North region of Brazil.

		Rain (mm/d)	Rain (mm)	*P* (mb)	*Rad* (kj/m²)	*T* med (ºC)	*T* min (ºC)	*T* max (ºC)	*dT* (ºC)	*RH* (%)	*W* med (m/s)	*W* max (m/s)
Rio Branco - AC	J	0.42	314.85	985	1152	25.21	24.77	25.68	19.06	86.35	1.40	3.82
	F	0.46	301.07	985	1173	25.25	24.80	25.72	19.22	87.02	1.16	3.41
	M	0.30	209.36	986	1143	25.30	24.84	25.79	22.12	86.89	0.98	3.03
	A	0.16	103.24	986	1209	25.38	24.89	25.90	21.52	83.12	0.90	2.75
	M	0.10	47.55	987	1173	24.85	24.35	25.43	20.61	80.47	0.77	2.36
	J	0.06	47.21	988	1257	24.72	24.18	25.31	14.49	64.12	0.85	2.61
	J	0.05	22.54	989	1441	25.13	24.44	25.97	16.16	62.28	1.47	3.50
	A	0.03	15.40	987	1444	26.73	25.91	27.61	17.62	60.84	1.82	4.23
	S	0.10	62.42	986	1322	26.65	25.94	27.39	19.66	68.64	1.79	4.23
	O	0.24	159.08	985	1376	26.20	25.60	26.82	21.39	77.06	1.73	4.20
	N	0.26	181.61	984	1347	25.74	25.22	26.31	22.16	81.92	1.75	4.21
	D	0.32	227.83	984	1248	25.21	24.73	25.69	22.35	85.27	1.71	4.19
Porto Velho - RO	J	0.39	280.79	993	1203	25.84	25.38	26.67	22.81	84.41	1.43	3.63
	F	0.46	301.75	993	1180	25.84	25.40	26.76	22.83	84.49	1.38	3.57
	M	0.53	372.14	994	1203	25.95	25.31	26.77	22.97	84.70	1.36	3.60
	A	0.24	162.00	994	1282	26.22	25.65	26.89	22.86	83.04	1.26	3.35
	M	0.19	137.65	997	1285	25.81	25.25	26.56	22.11	81.57	1.22	3.27
	J	0.05	31.02	1000	1378	25.57	24.95	26.36	21.06	78.55	1.11	3.01
	J	0.01	8.71	1002	1458	26.50	25.69	27.49	18.51	66.10	1.41	3.67
	A	0.06	33.95	1001	1410	27.20	26.23	28.16	18.58	64.01	1.42	3.74
	S	0.12	74.15	1001	1505	28.26	27.19	28.94	20.79	67.22	1.43	3.80
	O	0.21	152.43	998	1524	27.56	26.49	28.24	22.10	74.28	1.43	3.80
	N	0.28	196.32	995	1325	27.03	25.98	27.76	22.77	78.96	1.41	3.64
	D	0.48	220.88	995	1066	25.86	25.22	26.56	22.73	83.86	1.43	3.63
Palmas - TO	J	0.45	320.04	978	1258	25.94	25.04	26.83	21.22	76.76	1.31	3.65
	F	0.43	297.30	978	1220	25.83	25.08	26.81	21.11	76.88	1.31	3.72
	M	0.33	256.57	978	1222	26.10	25.40	26.98	21.42	76.99	1.17	3.43
	A	0.22	158.93	978	1282	26.77	26.06	27.67	21.32	74.01	1.19	3.41
	M	0.05	37.14	979	1364	27.30	26.51	28.22	19.44	64.91	1.31	3.63
	J	0.00	7.57	981	1463	27.13	26.23	28.15	15.90	53.46	1.82	4.65
	J	0.00	2.17	981	1511	27.39	26.43	28.49	12.95	44.03	2.18	5.39
	A	0.00	1.54	980	1593	29.21	28.27	30.27	11.06	35.13	2.52	6.14
	S	0.05	35.78	979	1573	30.35	29.48	31.26	13.04	38.95	2.28	5.70
	O	0.15	116.41	977	1474	29.05	28.23	29.96	17.73	55.25	1.55	4.32
	N	0.31	172.81	977	1258	27.06	26.35	28.09	20.73	70.60	1.36	3.81
	D	0.30	211.59	977	1216	26.48	25.78	27.47	20.98	73.57	1.33	3.74
Manaus - AM	J	0.33	234.71	956	1111	25.97	25.42	26.44	21.94	75.15	1.37	3.83
	F	0.31	208.10	955	1050	25.69	25.21	26.19	21.91	76.13	1.42	3.89
	M	0.43	291.86	955	1052	25.24	24.82	25.69	22.10	79.07	1.26	3.55
	A	0.34	248.56	957	1111	25.53	25.09	25.98	22.28	78.58	1.19	3.35
	M	0.26	172.59	963	1115	25.98	25.53	26.44	22.49	77.97	1.12	3.27
	J	0.17	113.17	964	1221	25.98	25.51	26.49	21.86	75.28	1.16	3.32
	J	0.08	67.27	964	1385	26.81	26.23	27.27	21.34	69.43	1.36	3.59
	A	0.07	50.98	963	1494	27.40	26.83	27.92	21.16	66.71	1.31	3.53

Table 1. (Continued)

		Rain (mm/d)	Rain (mm)	*P* (mb)	*Rad* (kj/m²)	*T* med (ºC)	*T* min (ºC)	*T* max (ºC)	*dT* (ºC)	*RU* (%)	*W* med (m/s)	*W* max (m/s)
Manaus	S	0.09	62.04	962	1325	27.32	26.78	27.89	21.42	68.22	1.25	3.49
	O	0.14	95.85	961	1254	27.20	26.71	27.76	21.75	69.99	1.32	3.61
	N	0.23	162.75	960	1202	27.08	26.56	27.58	22.18	72.06	1.31	3.53
	D	0.30	222.60	961	1075	26.16	25.67	26.64	22.34	76.55	1.24	3.46
Belém - PA	J	0.53	379.98	1008	4872	26.27	25.74	26.84	23.21	84.19	0.93	3.69
	F	0.64	435.95	1008	4221	25.91	25.41	26.45	23.26	86.15	0.84	3.42
	M	0.68	462.81	1009	4250	25.98	25.49	26.54	23.34	86.11	0.76	3.26
	A	0.57	388.34	1009	5449	26.24	25.73	26.82	23.54	86.00	0.74	3.17
	M	0.50	288.65	1009	6047	26.98	26.42	27.63	23.51	82.46	0.89	3.51
	J	0.30	145.36	1010	7518	27.55	26.96	28.20	22.91	77.11	1.01	3.74
	J	0.19	106.96	1010	8395	27.80	27.19	28.42	22.54	74.63	1.16	3.99
	A	0.21	123.25	1010	7271	27.67	27.08	28.35	22.65	75.56	1.17	4.32
	S	0.22	138.81	1009	6652	27.19	26.62	27.81	22.67	77.66	1.10	4.32
	O	0.24	49.56	1008	5637	27.23	26.66	27.86	22.78	77.92	1.09	4.31
	N	0.24	132.95	1000	5706	27.33	26.75	27.95	22.63	76.18	1.14	4.28
	D	0.43	231.98	1000	4947	26.71	26.10	27.24	23.04	80.48	0.98	3.77
Macapá - AP	J	0.28	202.08	1007	1281	26.47	25.72	26.61	22.65	81.25	1.85	4.86
	F	0.48	322.92	1001	1136	25.68	25.28	26.11	22.65	84.26	1.67	4.70
	M	0.48	360.01	1001	1157	25.91	25.52	26.34	22.92	84.15	1.60	4.43
	A	0.51	361.37	1007	1292	26.40	25.98	26.85	23.22	83.86	1.61	4.39
	M	0.48	356.38	1009	1278	26.49	26.08	26.94	23.31	83.83	1.53	4.12
	J	0.27	179.35	1010	1397	26.82	26.34	27.33	22.83	80.66	1.63	4.35
	J	0.12	142.65	1002	1558	26.88	26.37	27.41	22.36	77.12	1.77	4.64
	A	0.06	61.89	1001	1774	27.93	27.41	28.48	22.31	72.23	2.26	5.59
	S	0.10	73.61	1009	1737	28.54	27.78	28.83	22.37	70.75	2.46	6.09
	O	0.02	23.29	999	1905	28.44	27.94	28.99	22.10	69.23	2.71	6.33
	N	0.21	166.38	991	1677	27.69	27.23	28.20	22.39	72.82	2.43	5.81
	D	0.18	141.13	992	1480	26.92	26.46	27.41	22.47	76.45	2.12	5.36
Boa Vista - RR	J	0.03	18.38	1001	1584	28.14	27.49	28.79	19.52	61.39	2.44	6.42
	F	0.04	25.45	1001	1488	28.07	27.48	28.70	19.24	60.69	2.60	6.80
	M	0.07	35.98	1001	1528	28.53	27.93	29.18	19.58	60.52	2.36	6.28
	A	0.21	131.12	1002	1563	28.16	27.50	28.80	21.08	67.79	2.01	5.33
	M	0.34	257.99	1003	1356	26.87	26.30	27.48	21.95	75.81	1.59	4.39
	J	0.31	282.04	1003	1274	26.36	25.75	27.00	22.03	78.17	1.45	3.99
	J	0.27	245.80	1004	1212	25.91	25.30	26.55	21.96	80.06	1.31	3.61
	A	0.16	124.99	1003	1533	27.01	26.34	27.71	21.81	75.11	1.41	3.94
	S	0.15	125.22	1002	1727	28.03	27.32	28.75	21.27	68.87	1.54	4.18
	O	0.05	41.16	1000	1668	28.90	28.19	29.63	21.04	64.70	1.67	4.49
	N	0.06	37.33	1000	1598	28.73	28.06	29.43	21.09	65.72	1.79	4.80
	D	0.06	29.87	1000	1599	28.11	27.48	28.78	20.62	65.69	2.11	5.59

Legend: *P*= atmospheric pressure; *Rad*= incident solar radiation; *dT*= dew temperature; *RH*= relative humidity of air; *W*= wind.

Table 2. Frequency distribution of monthly rainfall averages by climate zone.

	Class		*x*	*f*	*cf*	*rf*	*crf*		Class		*x*	*f*	*cf*	*rf*	*crf*
AC	0.0	59.2	29.6	737	737	27.4	27.4	**PAc**	0.0	72.3	36.2	1019	1019	44.2	44.2
	59.2	118.4	88.8	617	1354	23.0	50.4		72.3	144.6	108.5	317	1336	13.8	58.0
	118.4	177.6	148.0	456	1810	17.0	67.3		144.6	216.9	180.8	403	1739	17.5	75.5
	177.6	236.8	207.2	429	2239	16.0	83.3		216.9	289.2	253.1	325	2064	14.1	89.6
	236.8	296.0	266.4	257	2496	9.6	92.9		289.2	361.5	325.4	152	2216	6.6	96.2
	296.0	355.2	325.6	149	2645	5.5	98.4		361.5	433.8	397.7	59	2275	2.6	98.7
	355.2	414.4	384.8	26	2671	1.0	99.4		433.8	506.1	470.0	21	2296	0.9	99.7
	414.4	473.6	444.0	13	2684	0.5	99.9		506.1	578.4	542.3	5	2301	0.2	99.9
	473.6	532.8	503.2	4	2688	0.1	100		578.4	650.7	614.6	3	2304	0.1	100
RO	0.0	64.8	32.4	878	878	32.7	32.7	**AMs**	0.0	67.9	33.9	328	328	14.2	14.2
	64.8	129.6	97.2	705	1583	26.2	58.9		67.9	135.7	101.8	476	804	20.7	34.9
	129.6	194.4	162.0	381	1964	14.2	73.1		135.7	203.6	169.6	492	1296	21.4	56.3
	194.4	259.2	226.8	311	2275	11.6	84.6		203.6	271.4	237.5	468	1764	20.3	76.6
	259.2	324.0	291.6	238	2513	8.9	93.5		271.4	339.3	305.3	287	2051	12.5	89.0
	324.0	388.8	356.4	133	2646	4.9	98.4		339.3	407.1	373.2	199	2250	8.6	97.7
	388.8	453.6	421.2	34	2680	1.3	99.7		407.1	475.0	441.0	43	2293	1.9	99.5
	453.6	518.4	486.0	6	2686	0.2	99.9		475.0	542.8	508.9	8	2301	0.3	99.9
	518.4	583.2	550.8	2	2688	0.1	100		542.8	610.7	576.7	3	2304	0.1	100
TO	0.0	67.9	33.9	3544	3544	46.1	46.1	**PAs**	0.0	97.9	49.0	1827	1827	39.6	39.6
	67.9	135.7	101.8	882	4426	11.5	57.6		97.9	195.8	146.9	926	2753	20.1	59.7
	135.7	203.6	169.6	1437	5863	18.7	76.3		195.8	293.7	244.8	882	3635	19.1	78.9
	203.6	271.4	237.5	1111	6974	14.5	90.8		293.7	391.6	342.7	586	4221	12.7	91.6
	271.4	339.3	305.3	499	7473	6.5	97.3		391.6	489.5	440.6	288	4509	6.3	97.9
	339.3	407.1	373.2	164	7637	2.1	99.4		489.5	587.4	538.5	80	4589	1.7	99.6
	407.1	475.0	441.0	27	7664	0.4	99.8		587.4	685.3	636.4	14	4603	0.3	99.9
	475.0	542.8	508.9	8	7672	0.1	99.9		685.3	783.2	734.3	3	4606	0.1	100
	542.8	610.7	576.7	8	7680	0.1	100		783.2	881.1	832.2	2	4608	0.0	100
AM*m*	0.0	86.6	43.3	813	813	30.2	30.2	**AP**	0.0	76.2	38.1	441	441	28.7	28.7
	86.6	173.1	129.8	650	1463	24.2	54.4		76.2	152.3	114.2	205	646	13.3	42.1
	173.1	259.7	216.4	579	2042	21.5	76.0		152.3	228.5	190.4	369	1015	24.0	66.1
	259.7	346.2	302.9	402	2444	15.0	90.9		228.5	304.6	266.5	172	1187	11.2	77.3
	346.2	432.8	389.5	159	2603	5.9	96.8		304.6	380.8	342.7	195	1382	12.7	90.0
	432.8	519.3	476.0	38	2641	1.4	98.0		380.8	456.9	418.8	106	1488	6.9	96.9
	519.3	605.9	562.6	29	2670	1.1	99.0		456.9	533.1	495.0	38	1526	2.5	99.3
	605.9	692.4	649.1	11	2681	0.4	100		533.1	609.2	571.1	6	1532	0.4	99.7
	692.4	779.0	735.7	7	2688	0.3	100		609.2	685.4	647.3	4	1536	0.3	100
PA*m*	0.0	81.6	40.8	2043	2043	40.9	40.9	**RR**	0.0	75.5	37.7	602	602	52.3	52.3
	81.6	163.1	122.3	883	2926	17.7	58.6		75.5	150.9	113.2	274	876	23.8	76.0
	163.1	244.7	203.9	1106	4032	22.2	80.8		150.9	226.4	188.6	59	935	5.1	81.2
	244.7	326.2	285.4	651	4683	13.0	93.8		226.4	301.8	264.1	71	1006	6.2	87.3
	326.2	407.8	367.0	215	4898	4.3	98.1		301.8	377.3	339.5	28	1034	2.4	89.8
	407.8	489.3	448.5	77	4975	1.5	99.7		377.3	452.7	415.0	60	1094	5.2	95.0
	489.3	570.9	530.1	10	4985	0.2	99.9		452.7	528.2	490.4	36	1130	3.1	98.1
	570.9	652.4	611.6	3	4988	0.1	99.9		528.2	603.6	565.9	14	1144	1.2	99.3
	652.4	734.0	693.2	4	4992	0.1	100		603.6	679.1	641.3	8	1152	0.7	100
AM*c*	0.0	63.5	31.7	418	418	15.6	15.6								
	63.5	126.9	95.2	728	1146	27.1	42.6								
	126.9	190.4	158.6	522	1668	19.4	62.1								
	190.4	253.8	222.1	531	2199	19.8	81.8								
	253.8	317.3	285.5	297	2496	11.0	92.9								
	317.3	380.7	349.0	140	2636	5.2	98.1								
	380.7	444.2	412.4	39	2675	1.5	99.5								
	444.2	507.6	475.9	10	2685	0.4	99.9								
	507.6	571.1	539.3	3	2688	0.1	100								

Legend: *m*= southern; *c*= central; *s*= northern; *x*= mean point, *f*= frequency; *cf*= cumulative absolute frequency; *rf*= relative frequency; *crf*= cumulative relative frequency (1991 – 2022).

In the southern zone, considering the total number of stations measured in the states of Acre, Rondônia and Tocantins, the highest frequency (*f*) of data is found at an average point numerically lower than 34 mm/month. In the southern region of Amazonas (southern zone – AM*m*) the highest frequency average point was 43.3 mm/month. In Pará, the southern (PA*m*) and central (PA*c*) climate zones, under the influence of a savanna environment and with interference from dry air masses from the Cerrado Biome, had the highest frequency of data, numerically lower than 41 mm/month. In the northeastern zone of the Pará (PA*s*), the highest frequency of data was for the midpoint 49.0 mm/month, while in Amapá (AP) this value was 38.1 mm/month. The greatest divergence of values was observed in the northwestern zone, where the State of Amazonas (AM*s*) had the highest frequency for an average precipitation of 169.6 mm/month, while in Roraima (RR) the average point was 37.7 mm/month for a high frequency of 602 units. The values represented by the following midpoints stood out with cumulative relative frequency (*crf*) above 90%: in the central-west region of the southern zone, 266.4 mm/month of rain in Acre, 291.6 mm/month in Rondônia and 237.5 mm/month in Tocantins.

For the southern zone of the states of Amazonas and Pará, average points were obtained for *crf* above 90% of 302.9 and 285.4 mm/month, respectively. In the central climate zone of Amazonas and Pará, the mean values for *crf* above 90% were 285.5 and 325.4 mm/month, respectively. In the northern climatic zone, moving along the E-W axis, the following midpoints were calculated: 342.7 in Pará and Amapá for 91.6 and 90% *crf*, respectively; 373.2 (97.7%) in Amazonas; and 415 mm/month of rain in Roraima for 95% (Table 2). Considering these values, the center-west region of the southern zone was the most conservative in terms of rainfall distribution. Most of the sample above 90% presented monthly precipitation between 244 and 346 mm/month, highlighting in the southern climate zone west of Amazonas, the stretch that comprises the municipalities of Letícia, Benjamin Constant, Eirunepé, Tefé, and from Coari to Manicoré region. Despite the great variability of the results, due to the great climatic oscillation, the analyses of absolute, relative and accumulated frequency of rainfall proved to be important for the recognition of the distribution of sample values in space (zoning), identifying the areas of greater and lesser precipitation according to rainfall records.

In view of the fact that the climatic variables do not behave as independent and equally distributed random variables, it was decided to apply the principle of likelihood. This principle states that your function (*fx*) contains all information about an unknown parameter in the data. The value of this parameter tends to maximize the probability of numerically obtaining the most likely sample, being quite suitable for large samples with high variability, which graphically represent a high asymmetry, as was the case in this study. Table 3 presents the result of the Gamma distribution analysis, with the estimated values of the α and β parameters for the established climatic zones. The parameters were calculated based on the analysis of monthly precipitation values from 1991 to 2022, for the weather stations of each state and/or climate zone, graphically represented in Figure 2. The α values ranged from 0.90 in the Roraima region to 3.23 for the northern Amazon (AM*s*) climate zone. The low values calculated for the α parameter bring security to the application of the Gamma distribution model for the monthly analysis. The β parameter values ranged from 57.42 to 145.29 mm, with a predominance of values close to 100 mm. The high results are due to the high variance determined, a consequence of the significant difference in precipitation between the rainy and dry months. In this condition, there was no evident pattern of spatial similarity between the studied climate zones. The K-S adherence test allowed for estimating the obtained values (D_o) slightly lower than the respective critical values (D_{cr}) obtained in the table for each validated sample number (*n*). This means that there is agreement between the observed and expected frequencies for the consulted historical series.

Table 3. Gamma distribution alpha (α) and beta (β) parameters and Kolmogorov-Smirnov adherence test (5%) for monthly rainfall in climate zones.

	n	*X*	*m*	*S*	S^2	α	β	K-S D_o	K-S D_{cr}
AC	2688	136.2	116.2	97.3	9460.9	1.96	69.45	0.025	0.026
RO	2688	129.9	103.3	107.9	11632.4	1.45	89.55	0.024	0.026
TO	7680	114.3	87.2	108.7	11810.8	1.11	103.31	0.014	0.016
AM*m*	2688	173.5	159.3	127.4	16226.3	1.86	93.52	0.022	0.026
PA*m*	4992	137.8	127.6	114.6	13128.8	1.45	95.26	0.017	0.019
AM*c*	2688	162.6	148.6	96.6	9338.1	2.83	57.42	0.019	0.026
PA*c*	2304	133.0	99.7	115.1	13241.8	1.34	99.57	0.025	0.028
AM*s*	2304	191.6	184.8	106.6	11359.6	3.23	59.29	0.013	0.028
PA*s*	4608	175.3	136.4	138.5	19176.6	1.60	109.42	0.018	0.020
AP	1536	187.1	171.2	136.9	18743.9	1.87	100.16	0.031	0.035
RR	1152	130.1	71.5	137.5	18903.9	0.90	145.29	0.036	0.040

Legend: *X*= mean; *m*= median; D_o= observed value; D_{cr}= critic value.

3.3 Seasonal analysis of climate zones

Inferential statistics is based on the Theory of Probability and Sampling within a sampling universe. Among the most commonly applied probability distributions are Student's *t* (Gosset), Fisher-Snedecor's *F* and Pearson's chi-square, important techniques not only for hypothesis testing, but also for analysis of variance and regression. The patterns of occurrence and distribution of meteorological phenomena can be predicted in probabilistic terms through the use of theoretical distribution models, with probability density functions adjusted to a historical series. In this sense, among the distribution models available from frequency histograms, the incomplete Gamma distribution model with *Fx* density function has shown good results in estimating probabilities and simulating daily climate data [23,29,31-33].

From the analysis of daily and monthly data, as well as the results summarized in Tables 1 and 2, the regional seasonality was established for each of the seven states that make up the study area. In general, considering the monthly average and standard deviation of precipitation for the period from 1991 to 2022, it was observed that the number of rainy days with significant precipitation predominated in relation to dry days or days of low precipitation for the hydrological cycle analyzed. During the most significant months of drought, precipitation ranged from 0.0 or no monthly rainfall to 99.8 mm/month, recorded for July 2017 in the municipality of Maués (AM). Within this scenario, the most evident drought in regional terms was observed in Tocantins, with annual records of no rain between June and August. Contrary to the more homogeneous pattern observed during the periods of maximum drought, the rainy periods were marked by a greater oscillation of the results. Mean monthly precipitation values for the rainy season ranged between 238 mm/month in Tocantins and 301 mm/month in Roraima. The difference between the minima and maxima also had greater amplitude of space-time variation. While in the dry season the difference between maximums and minimums was less than 100 mm/month, in months of intense rains the difference ranged between 445 mm in Acre and 711 mm in Pará.

The results presented in Table 4 summarize the seasonally observed values by state and period. The central tendency (position) and dispersion measures calculated confirmed the proposed trend of seasonal zonation, significantly differentiating dry and rainy periods. It

should be considered that in Pará and Tocantins, due to their respective locations, there is a direct influence of dry air masses originating from the Cerrado, attenuating the volume of local precipitation. The existing intersection between the sub-basins of the Amazon River, especially in the center-east of the North region, with the Tocantins-Araguaia basin, establishes a scenario of transition or zonation in the climatic and physiographic aspect, with transitions between dense forest, open forest and savanna. Despite the trend of moments of greater annual precipitation, it was not possible to establish a conservative condition for the entire study region due to the large territorial extension and the significant nuances of precipitation, especially in the E-W axis of the northern climate zone. A review of historical data associated with climate projections for the Amazon suggests that there has been an overestimation of precipitation data, especially for the rainy seasons in the northeastern climate zone (PAs and AP).

Table 4. Central tendency and dispersion measurements of the precipitation for periods of maximum drought and rainfall in north region.

	AC	RO	TO	AM	PA	AP	RR
				Dry period			
X	36.8	22.2	9.0	41.0	35.1	37.2	33.9
m	32.6	12.0	1.9	39.6	32.2	31.5	35.4
S	21.9	22.8	14.8	25.8	24.5	25.8	20.5
S^2	479.5	519.3	219.9	664.4	599.5	664.8	420.6
min	0.0	0.0	0.0	0.0	0.0	0.0	0.0
max	97.8	96.8	88.2	99.8	99.2	96.8	91.3
				Rainy period			
X	241.9	274.3	238.3	271.0	286.2	300.4	300.9
m	236.8	272.2	232.1	262.8	277.4	288.9	290.4
S	74.1	82.7	74.0	90.6	105.3	99.7	119.5
S^2	5488.2	6837.3	5479.2	8216.3	11086.3	9946.4	14268.5
min	87.8	84.6	33.4	37.9	22.4	100.0	74.8
max	532.4	583.0	610.4	714.5	733.6	685.2	679.0

From the perspective of distribution and normality analysis, the values of the α and β parameters were estimated for the incomplete Gamma distribution. The α parameter, estimated by the likelihood method, confirmed the possibility of using the Gamma distribution model in seasonal conditions for the climatic phenomena of the study area. Values ranged from 0.36 to 11.0 (Table 5), well below the safety limit established by Thom [23], who considered that the application of the incomplete gamma distribution model was not recommended in cases of α values greater than 100. The lowest values of α occurred in the southern climate zone; however, it is not possible to differentiate these indices for the dry and rainy periods of the respective climate zone. Values for the β parameter varied between 12.4 and 47.4 mm, with the highest rates (> 30 mm) being observed in the northeastern climatic zone, in the State of Amapá, and in the northwestern zone in Roraima. Based on the estimated α and β parameters, the results suggest a good possibility of using the Gamma distribution model to determine different levels of probability in the climatic zones and sub-regions of the study area. Several studies have confirmed this trend of applying the Gamma model, whose results have shown good fit and efficiency for the data set, especially in determining monthly precipitation totals, estimating probabilities, and simulating daily, monthly or annual climate data [32-36].

From the applied approach, considering the monthly, seasonal (drought and rains), and annual analyses, it is reinforced that the chosen model can be used in the study of the behavior of meteorological parameters in different regions, regardless of the size of the historical series. This is an important characteristic, since despite its value in the regional and global climatic context, the study of historical series in the North region presents difficulties with the insufficiency and discontinuity of data. During this study, 'empty' geographic spaces of information were identified, due to the absence of climatological stations or lack of continuity in the measurement. Two subareas where the presence of these empty spaces is evident are the northern limit of the North region, close to the border area with Venezuela and Guyana, and the northwestern zone in the State of Amazonas, between the municipalities of São Gabriel da Cachoeira (AM) and Cruzeiro do Sul in Acre (Fig. 1). This absence or discontinuity of information frequency can limit the climate analysis of a given region, interfering with environmental preservation studies, agricultural productivity logistics and the rational use of available natural resources [37].

Table 5. Gamma distribution alpha (α) and beta (β) parameters and Kolmogorov-Smirnov (5%) adherence test for seasonal rainfall, with probability levels from 10 to 90% of precipitation.

					K-S (p<.01)		Probability levels (%)				
	X	S^2	α	β	D_o	D_{cr}	90	75	50	25	10
AC*d*	36.8	479.5	2.82	13.04	0.050	0.056	10.6	17.7	32.6	51.7	67.2
RO*d*	22.2	519.3	0.95	23.40	0.061	0.068	0.6	6.1	12.0	34.8	57.5
TO*d*	9.0	219.9	0.36	24.56	0.029	0.033	0.0	0.1	1.9	11.4	28.5
AM*d*	41.0	664.4	2.53	16.19	0.031	0.034	10.8	17.3	39.6	61.0	79.0
PA*d*	35.1	599.5	2.06	17.07	0.024	0.027	5.2	14.0	32.2	52.0	73.0
AP*d*	37.2	664.8	2.09	17.85	0.057	0.063	5.9	18.2	31.5	56.3	77.6
RR*d*	33.9	420.6	2.73	12.42	0.090	0.100	9.1	17.6	35.4	45.0	64.0
AC*r*	241.9	5488.2	10.66	22.69	0.050	0.056	149.6	190.5	236.8	290.4	335.7
RO*r*	274.3	6837.3	11.00	24.93	0.061	0.068	175.6	222.7	272.2	325.0	387.8
TO*r*	238.3	5479.2	10.36	23.00	0.029	0.033	150.3	188.4	232.1	281.1	334.0
AM*r*	271.0	8216.3	8.94	30.32	0.031	0.034	157.8	209.3	262.8	324.0	382.2
PA*r*	286.2	11086.3	7.39	38.73	0.024	0.027	159.2	206.6	277.4	345.8	436.6
AP*r*	300.4	9946.4	9.07	33.11	0.057	0.063	170.8	220.8	288.9	357.4	432.8
RR*r*	300.9	14268.5	6.35	47.42	0.090	0.100	138.2	221.2	290.4	382.7	411.6

Legend: *d*= drought and *r*= rainy periods.

Estimates within a wide historical series can be established with probability estimation precision. According to [24], distribution models accompanied by specific adherence tests, such as the Kolmogorov-Smirnov or K-S test, allow comparing the empirical probabilities of a variable with the critical probabilities estimated by the distribution function. This comparison between probabilities allows checking whether the sample values can be derived from the population of the theoretical distribution. The K-S test is based on the magnitude of the greatest difference between the observed and estimated probability, with the cumulative aspect of errors not occurring. The K-S values obtained (D_o) for the seasonal moment were lower than the critical values (D_{cr}) for 5% (Table 5), suggesting that there is agreement between the observed and expected frequencies, as well as a good fit of the Gamma distribution for the historical series of precipitation data applied to the model. The smallest difference between the obtained K-S and the tabulated value was observed in Pará, while the largest difference was determined in Roraima. The Gamma distribution obtained great adherence by the K-S test. The results allowed us to consider that the Gamma probability

distribution function was adequate to represent precipitation for monthly and seasonal periods (drought and rainy). From a space-time perspective, in the months with the highest occurrence of precipitation, the average rainfall remained between levels of 25 and 50% probability. This trend continued for the dry season, established between the months of July and September for most states in the North region. The exception was Roraima, whose dry period fell between November and March. In this case, the average occurrence of rainfall increased to levels of 50 to 75% probability, suggesting that in the months of lower precipitation, the temporal variation is less accentuated, with a greater probability of occurrence of values above the average.

3.4 Annual climate projection

Within the space-time perspective, the climatic zones were classified and grouped as follows: in the southern zone – Acre, Rondônia, Tocantins and southern portion of Amazonas (AM*m*); in the central zone – Amazonas (AM*c*) and Pará (PA*c*); in the northeastern climatic zone – Pará (PA*s*) and Amapá; and in the northwestern zone – part of Amazonas (AM*s*) and Roraima. Once the precipitation zones were identified, the distribution of average annual rainfall (Fig. 3A) and the frequency of class distribution (Fig. 3B) by zonation were established. Especially the monitoring stations located in Roraima and in the climatic zones of Amazonas and Pará had greater fluctuation in annual averages for the study period. Some of these oscillations result directly from the influence of global meteorological phenomena. Others, however, derive from punctual and regional events, such as cold phenomena (*friagem*) or changes in the intensity and direction of warm and humid air masses coming from the ocean. The highest annual rainfall for the period 1991 – 2022 was observed in the AM*s* sub-regions, with an average of 2299±99 mm/year; AP averaging 2246±86 mm/y and PA averaging 2103±112 mm/y, all in the northeast climate zone. The lowest annual rainfall was observed in Tocantins (1371±68 mm/y) and Rondônia (1558±85 mm/y; Fig. 3A). The trends and behavior of annual oscillation were confirmed in the class frequency histogram (Fig. 3B), highlighting the average values above 2100 mm/y representing 72% of the sample for AM*s*, and 69% for AP and PA*s*. A second group also stood out with an absolute frequency close to 66% for AC, RO and TO, all belonging to the southern zone.

The climate of the Amazon is the result of the interaction of regional phenomena, attributed to the hydrological cycle in the Amazon Biome, and global events, involving the movement of large air masses such as mEc, ITCZ, TIL, AB and ENSO. In this regard, monitoring the intensity and direction of the winds is essential for understanding the patterns of displacement of air masses in the region. From the determination of the direction and intensity of the annual winds between 1991 and 2022, a distribution model of the predominant winds in the North region was established (Fig. 4). The model result suggests that, from a vector point of view, the predominant winds in the region come from the east throughout the annual cycle, with two components: one in the E-W direction and the other SE-NW. About the maximum intensity of the winds, the values varied as follows: in the southern section, from 0.0 to 25 m/s (average 5.7±4.7 m/s) in Acre; up to 42 m/s (average 6.7±5.3 m/s) in Rondônia; in the Tocantins State, up to 39 m/s (7.2±5.4 m/s); 33 m/s (5.5±4.9) in Amazonas, and 36 m/s (6.2±5.1 m/s) in Pará. In the central area of the Amazon, values ranged from 0 to 99 m/s (average 6.4±7.3 m/s) in the State of Amazonas and 24 m/s (6.6±4.9 m/s) in the Pará. In the northern climatic zone, the maximum values were 24 m/s (5.6±4.3 m/s) in Roraima; 23 m/s (5.8±4.0 m/s) in Amapá; 21 m/s (5.5±4.8 m/s) in Amazonas and 31 m/s (5.3±4.6 m/s) in Pará. The results suggest greater stability and constancy in the annual winds in the northern zone, where the higher relief in the Guiana and Cristalino Shields, as well as in the northwest area with the Pre-Andean region, acts as a natural physical barrier to movement of the air masses. The results corroborate studies carried out

in the Amazon, which claim that winds from the Eastern Amazon towards the Andes transport large amounts of water vapor, which extend to the South and Southeast of South America, constituting the main source of humidity for these regions [5,15,38].

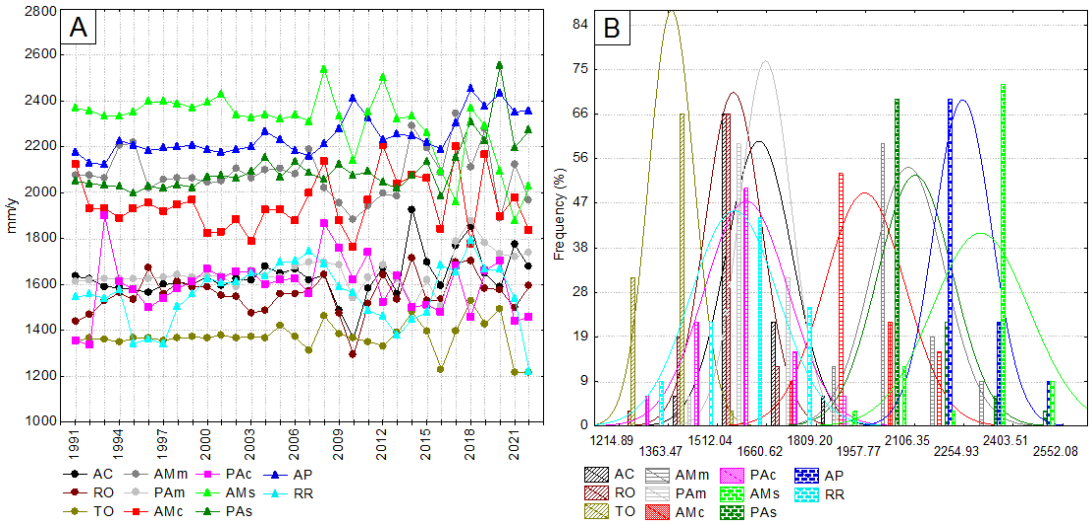

Fig. 3. A) Average annual distribution of rainfall and B) Class frequency histogram for the seven states in the North region of Brazil. Legend: *m*= southern; *c*= central and *s*= northern zone.

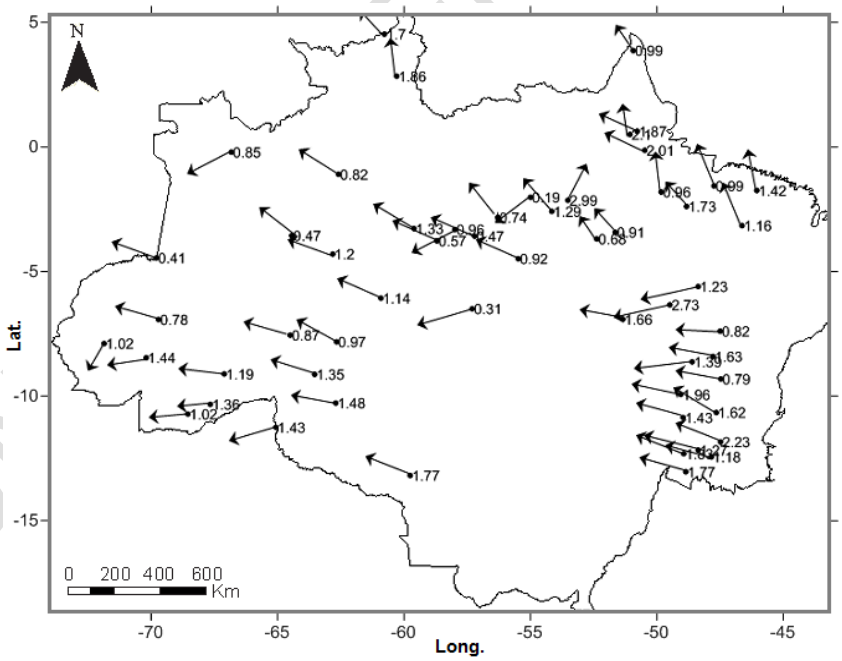

Fig. 4. Model of direction and intensity of annual winds for the North region of Brazil based on data analyzed between 1991 and 2022. (Legal Amazonian Map generated in ArcGis® 9.3 ©2008).

3.5 Image Interpolation

The application of the Geographic Information System (GIS) in climatological studies has contributed to a more reliable space-time representation of the results, allowing a greater approximation between the models and the regional climate reality. Several techniques have been applied to identify the spatial-temporal precipitation pattern, including the application of arithmetic, geometric and weighted means; Thiessen polygons; variograms and inverse distance interpolation (IDW), the latter of which is recommended in cases of obtaining continuous and heterogeneous maps. The analysis of seasonal rainfall distribution and variability has been increasingly studied within the Brazilian territory, due to its wide applicability [39,40].

The space-time distribution of annual precipitation for the study period allowed the establishment of four distinct climatic regions (quadrants): south, central, northeast and northwest regions (Fig. 5). The lowest average annual values were observed in the southern region, which included the states of Acre, Rondônia, Tocantins, and part of Amazonas (AM*m*) and Pará (PA*m*), with annual values oscillating between 1489 – 1814 mm/y. This quadrant is marked by the association with the Cerrado Biome and its respective climatic and physiographic influences. Following are the average annual precipitations of the central region, which includes the states of Amazonas (AM*c*) and Pará (PA*c*), with an interval between 1616 – 2001 mm/y. The highest precipitation values were observed in the northwest (NW), in Roraima and Amazonas (AMs), with minimum and maximum values between 1625 – 2114 mm/y, and in the northeast (NE) in Amapá and Pará (PA*s*), with an interval between 2077 – 2492 mm/y. The NE quadrant had the highest precipitation values, both punctual and average, despite being located closer to the 'arc of deforestation', an area continuously devoid of native forest, which consequently has a strong negative influence on precipitation. It should be noted that the south, central and northwest regions maintained a regular oscillation pattern within the analyzed period, with a slight reduction in precipitation in the NW region. The values of the coefficients of variance (R^2) confirm the respective trends.

Despite proposing slightly higher precipitation values in their study, Ishihara et al. [9] when studying spatially and quantitatively the precipitation in the Legal Amazon, between 1978 and 2007, obtained a trend of distribution by quadrants very similar to that obtained in this research. The NE quadrant showed a tendency to increase the volume of precipitation over the years, especially from 2016 onward. This behavior can also be noted in the study by [9], although with less intensity, indicating an increase in the volume of rainfall in the last few years for the NE and NW quadrants and a decreasing pattern for the SE and SW quadrants. This increase in the volume of precipitation in recent years may result from the natural tendency due to the increase in warm and humid air masses brought from the ocean or, as already suggested, an overestimation of the results of maximum precipitation, which generates projections of increased climate instability in the region. As suggested by Tucci and collaborators [41], a time series of precipitation data will have a homogeneous pattern if the variations are caused by time and climate, that is, from natural conditions, since the homogeneity is represented by a series of climate data that have variations caused by physical characteristics. However, if there is interference of non-climatic factors in the distribution of precipitation, the homogeneity of the values will be affected, resulting in a gradual tendency of the data or a discontinuity in the variance. An example of this could be the process of deforestation of native forests for urban or agricultural expansion. Urbanization modifies the local climate, directly interfering with phenomena such as precipitation, winds (intensity and direction), humidity and temperature.

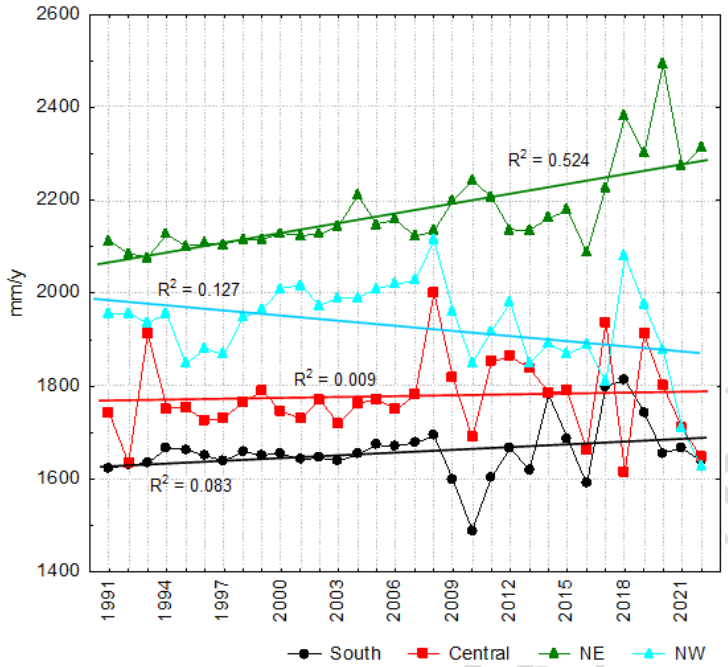

Fig. 5. Average annual rainfall per quadrant in the North region of Brazil for the historical series from 1991 to 2022.

The image interpolation maps of rainfall, temperature and relative humidity, from a space-time perspective for the North region are shown in Fig. 6. It was evident that climate variety had a direct cause-and-effect relationship with the physiography of the Amazon region. The highest annual rainfall was confirmed for the northern zone W and E (Fig. 6-A1). In the same way, the highest monthly precipitations in the dry season (Fig. 6-A2) and rains (Fig.6-A3) were also recognized in the northern climate zone E, especially in the area covering the Belém Metropolitan Region (PA). The dry periods were more intense in the southern zone, in the axis between Rondônia (W) and Tocantins (E). Relative air humidity followed the same behavior observed for precipitation, with high percentage rates for the northeastern zone (Figs. 6 C1-C3). The air temperature, on the other hand, showed its own oscillation pattern, with annual maximums (Fig. 6-B1) established for a large area located in the northwestern climate zone. This can be explained by the displacement of warm and humid air masses from the Atlantic Ocean towards the Pre-Andean and Andean regions.

The behavior of spatial-temporal continuity of precipitation, especially in the Amazon River basin, can be identified by the constancy of the average rainfall rates both in the headwaters and in the middle course of the basin, especially in the stretch comprised in the State of Amazonas. The highest continuous levels of precipitation in the northeast zone, especially at the mouth of the Amazon River, contribute to a regular event in the basin called '*repiquete'* which reflects a brief change in direction or in the rhythm of water level variation. It can occur both in ebb and in flood. In this condition, there is a *functional shutdown* and/or reversal of the ebb or flood for a quick return to the cycle phase. It occurs, respectively, when there is an increase or decrease in local rainfall or in the tributary watersheds.

Naturally, there are punctual and regional divergences in climate variability, especially precipitation, and in a region as extensive as the Amazon. When mapping a climate variable based on monitoring stations, the question of generalizing the result from specific samples must be taken into account. According to [42], precipitation presents a certain degree of

spatial dependence, so geostatistics related to the theory of regional variables becomes an alternative in sample analysis. This allows establishing, for example, an area of dependency between the variable and the monitored region. For the authors, a criterion applied in this context is that samples that are spatially closer tend to be more similar to each other. In this respect, the semivariogram is a fundamental mathematical function in the application of geostatistics, allowing the determination of the degree of dependence between two random variables in space and time, taking into respects the autocorrelation as a function of the distance and direction of the variables. If there is a certain degree of dependence between the samples, it is possible to estimate values for locations not sampled from the application of interpolation tests by kriging and/or cokriging, as demonstrated by [42-45].

These are important geostatistical tools applied in situations of discontinuity of historical series or in the presence of 'empty spaces' within the monitored area, as evidenced in this research. When establishing a spatial inference at a data discontinuity point, based on the estimation of neighboring samples, kriging unifies the sampling, expressing it in the semivariogram without trends, minimum variance and an acceptable confidence interval. These conditions corroborate the hierarchical grouping technique established by Ward's [26] minimum variance method. According to studies by [42,46], the kriging technique makes it possible to calculate a measure of the estimation error for each value in a confidence interval. The differential of this technique for cokriging is that it is a multivariate method that allows estimating several regional variables simultaneously based on the spatial correlation between them, which is fundamental to its use in the verification of the existing correlation between the primary variable and the secondary variables [27].

This study identified both a correlation between precipitation and humidity, as well as the distribution of rainfall and spatial zonation, certainly influenced by altitude (relief). In addition, sample discontinuities or empty spaces were identified in Figure 2. The measures of central tendency and dispersion calculated for annual and seasonal precipitation were close to those found in kriging interpolation. For these reasons, the ordinary kriging test proved to be satisfactory for data interpolation. The semivariograms were tested for the theoretical models, and the best result for the climate analysis, interpolated by kriging, was by the spherical linear model. Despite this, the Gaussian semivariogram theoretical model showed good results in the annual and monthly interpolation of precipitation by cokriging. The covariance calculated in the four horizontal directions, according to recommendations by [27], did not show significant differences, considering the isotropic semivariogram. The most significant result in this regard was the model established for the direction and intensity of the annual winds for the northern region (Fig. 4). The analysis of the distribution of climatic variables, especially precipitation, was regionally similar to that found by other studies, with slight discrepancies depending on the interval of the historical series as well as the scope of the study area.

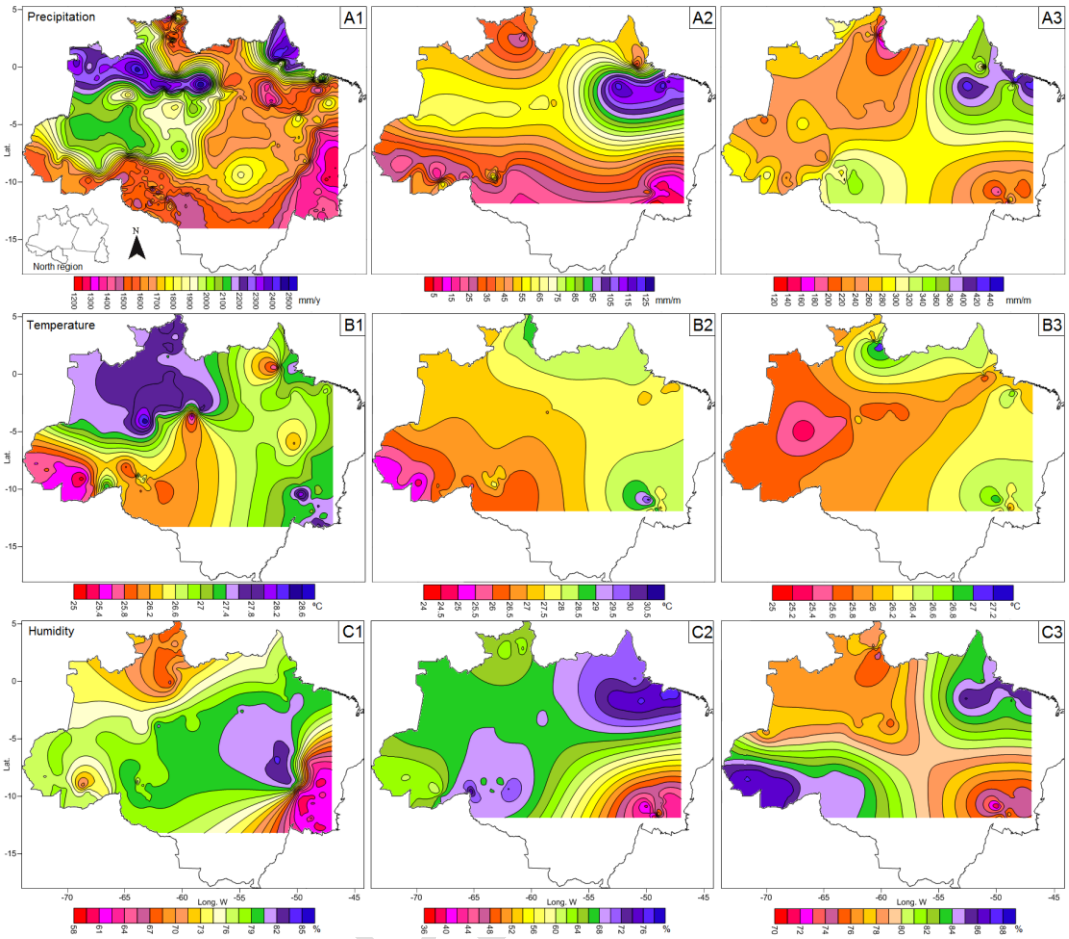

Fig. 6. Spatio-temporal variation of the A) precipitation, B) temperature and C) relative humidity of air for annual (1); drought (2); and rainy (3) seasonal periods by interpolation of data from meteorological stations, satellite estimates and conjunction of primary data from historical series from 1991 to 2022.

4. CONCLUSION

From the point of view of rainfall distribution, it was possible to establish four climatic zones with different rainfall regimes: southern, central, northwestern and northeastern. The results suggest a trend in the number of days with precipitation between 25 and 50% in most of the southern and central areas, and an increase in precipitation of 50 to 75% probability for the northern region. Despite this, it is considered that there was an overestimation of the secondary precipitation data, especially for the northeastern zone. Not all trends were statistically significant. The positive trend identified in the northwestern zone suggests an increase in rainfall events, especially in the last two decades. The exploratory analysis contributed to a better understanding of the climate distribution in the North region, considering the possibility of continuing to use the Gamma distribution model to interpret the historical series. Considering the behavioral similarity between precipitation and relative humidity, as well as the sample discontinuity identified in certain subareas, the ordinary kriging test was chosen for data interpolation. Among the semivariograms tested for the theoretical models, the one applied was the spherical linear model, although the Gaussian model also had a good response, in this case for the cokriging test. The results contributed

to a better understanding of the distribution of rainfall in the Amazon region, especially in the northern region of Brazil, which comprises about 90% of the Amazon Biome and 77% of the Brazilian Legal Amazon.

CONSENT

All the authors accepted the terms for publication, and we agree that, if the manuscript is accepted for publication, we'll transfer the copyright-holder of the manuscript to Journal of Geography, Environment and Earth Science International 2454-7352 – JGEESI, including the right of total or partial reproduction in all forms and media. We informed also that if accepted, the manuscript will not be published elsewhere including electronically in the same form, in English or in any other language, without the written consent of the copyright holder.

ETHICAL APPROVAL

This section is not applicable in this manuscript.

REFERENCES

1. Salati E, Vose PB. Amazon Basin: a system in equilibrium. Science. 1984; 225:129-138. https://doi.10.1126/science.225.4658

2. Molion LCB. Dynamic climatology of the Amazon region: precipitation mechanisms. Revista Brasileira de Meteorologia. 1987; 2(1):107-117. (Portuguese)

3. Fisch G, Marengo JA, Nobre CA. A general revision on the climate of the Amazon. Revista Acta Amazônica. 1998; 22(2):101- 126. (Portuguese)

4. Marengo JA, Nobre CA, Culf AD. Climatic impacts of "friagens" in forested and deforested areas of the Amazon basin. Journal of Applied Meteorology. 1997; 36(11):1553-1556.

5. Nobre CA, Obregón GO, Marengo JA, Fu R, Poveda G. Characteristics of Amazonian climate: main aspects, Geophysical Monograph Series. 2009; 186:149-162. https://doi.10.1029/2008GM000720 (Portuguese)

6. Davidson EA, de Araüjo AC, Artaxo P, Balch JK, Brown IF, Mercedes MM, Coe MT, DeFries RS, Keller M, Longo M, Munger JW, Schroeder W, Soares-Filho BS, Souza CM, Wofsy SC. The Amazon basin in transition. Nature. 2012; 481:321–328.

7. Sousa AML, Rocha EJP, Vitorino MI, Souza PJOP, Botelho MN. Spatio-temporal variability of precipitation in the Amazon during ENSO events. Revista Brasileira de Geografia Física. 2015; 8:15–29. https://doi.org/10.26848/rbgf.v8.1.p013-024 (Portuguese)

8. Silva DD, Pereira SB, Pruski FF, Gomes Filho RR. Rainfall intensity duration frequency equations for the state of Tocantins. Revista Engenharia na Agricultura (Viçosa). 2003; 11(1):7-14. (Portuguese)

9. Ishihara JH, Fernandes LL, Duarte AAM, Duarte ARCLM, Ponte MX, Loureiro GE. Quantitative and spatial assessment of precipitation in the Brazilian

Amazon (Legal Amazon) – (1978 to 2007). Brazilian Journal of Water Resources. 2014; 19(1):29-39.

10. Moraes BC, Sodré GRC, Souza EB, Ribeiro JBM, Meira Filho LG, Ferreira DB da S, Oliveira, J.V. Precipitation climatology in the Amazon. Revista Brasileira de Geografia Física. 2015; 8(5):1359-1373. https://doi.org/10.5935/1984-2295.20150074 (Portuguese)

11. Salviano MF, Groppo JD, Pellegrino GQ. Trend analysis in precipitation and temperature data in Brazil. Revista Brasileira de Meteorologia. 2016; 31(1):64-73. (Portuguese)

12. Azevedo FTM, Souza EB, Franco VS, Souza PFS. Seasonal forecast of regionalized precipitation in the Eastern Amazon. Revista Brasileira de Geografia Física. 2017; 10(5):1520-1534. (Portuguese)

13. Hastenrath S, Lamb P. Climate Atlas of the Tropical Atlantic and Eastern Pacific Oceans. University of Wisconsin Press, Madison, WI. 1977.

14. Geological Survey of Brazil [SGB/CPRM]. Hydrological and Hydrogeological Monitoring. Ministry of Mines and Energy, Secretariat of Geology, Mining and Mineral Transformation. Accessed on Nov. 12 2023 from http://www.cprm.gov.br/publique/Hidrologia/Monitoramento-Hidrologico-e-Hidrogeologico-366 (Portuguese)

15. Marengo JA, Nobre CA. Climate of the Amazon region. In: Cavalcanti IFA, Ferreira NJ, Da Silva MGAJ, Silva Dias MAF (Orgs.). Weather and Climate of Brazil. São Paulo: Oficina de Textos. 2009; 197-212. (Portuguese)

16. National Water Agency [ANA]. National Hydrometeorological Network. HIDRO System – Telemetry. Accessed on Oct. 18, 2023 from http://www.snirh.gov.br/hidrotelemetria/Mapa.aspx (Portuguese)

17. National Water Agency [ANA/Hidroweb]. Historical Season Series. Hidroweb, v.3.2.7. Accessed: on Oct. 16, 2023 from https://www.snirh.gov.br/hidroweb/serieshistoricas (Portuguese)

18. Brazilian Institute of Geography and Statistics [IBGE]. Legal Amazon. Accessed on Oct. 18, 2023 from https://www.ibge.gov.br/geociencias-novoportal/informacoes-ambientais/geologia/15819-amazonia-legal?=&t=sobre (Portuguese)

19. National Institute for Space Research [INPE/CPTEC]. (2016). Weather Prevision Center and Climate Studies. Accessed on Oct. 19, 2023 from http://enos.cptec.inpe.br and https://www.cptec.inpe.br (Portuguese)

20. National Institute of Meteorology [BDMEP/INMET]. INMET Portal. Accessed on Oct. 17, 2023 from https://portal.inmet.gov.br/dadoshistoricos (Portuguese)

21. National Department of Transport Infrastructure [DNIT]. (2018). Waterways. Brazilian waterways. Accessed on Oct. 22, 2023 from https://www.gov.br/dnit/pt-br/assuntos/aquaviario/intervencao-em-hidrovias/hidrovias-1 (Portuguese)

22. Faria RT, Caramori PH, Chibana EY, Brito LRS. Climate – Computer program for organizing and analyzing meteorological data. Engenharia Agrícola, Jaboticabal. 2003; 23(2):372-387. (Portuguese)

23. Thom HCS. A note on the Gama distribution. Monthly Weather Review, Washington. 1958; 86(4):117-122.

24. Assis FN, Arruda HV, Pereira AR. Applications of statistics to climatology: theory and practice. Pelotas, RS: Universidade Federal de Pelotas. 1996; 161p. (Portuguese)

25. Green PE. Analyzing multivariate data. Hinsdale, The Dryden Press, Illinois. 1978; 519p.

26. Ward JH. Hierarchical grouping to optimize an objective function. Journal of the American Statistical Association. 1963;58:236-244.

27. Yamamoto JK (2013) Geostatistic: concepts and applications. In: Yamamoto JK, Landim PMB (Eds.). Oficina de Textos, São Paulo. (Portuguese)

28. Santos JWMC. Climate Rhythm and Socio-Environmental Sustainability of Commercial Soybean Agriculture in Southeast Mato Grosso. Magazine of the Department of Geography (USP). 2005; 1:1-20. (Portuguese)

29. Dallacort R, Freitas PSL, Gonçalves ACA, Faria RT de, Resende R, Bertonha A. Yield probability levels of four soybean cultivars on five sowing dates. Acta Scientiarum Agronomy. 2008; 30(2):261-266. (Portuguese)

30. Centeno AJ. Statistics Applied Study to Biology. 1981; Didactic Collection 3, n. 49, Ed. UFG, Goiás. (Portuguese)

31. Suleiman AA, Ritchie JT. Modifications to the DSSAT vertical drainage model for more accurate soil water dynamics estimation. Soil Science. 2004; 169(11):745-757.

32. Murta RM, Teodoro SM, Bonomo P, Chaves MA. Monthly rainfall in probability levels by gamma distribution for two locations in southwestern Bahia. Science and Agrotechnology. 2005; 29(5):988-994. (Portuguese)

33. Lima JSS, Silva SA, Oliveira RB, Cecílio RA, Xavier AC. Temporal variability of monthly precipitation in Alegre – ES. Agricultural Science Magazine. 2008; 39(2):327-332. (Portuguese)

34. Araújo WF, Júnior ASA, Medeiros RD, Sampaio R. Probable monthly rainfall in Boa Vista, State of Roraima, Brazil. Brazilian Journal of Agricultural and Environmental Engineering. 2001; 5(3):563-567. (Portuguese)

35. Catalunha MJ, Sediyama GC, Leal BG, Soares CP, Ribeiro AB. Application of five probability density functions to rainfall series in the State of Minas Gerais. Brazilian Journal of Agrometeorology. 2002; 10(1):153-162. (Portuguese)

36. Sampaio SC, Queiroz MMF, Frigo EP, Longo AJ, Suszek M. Estimation and distribution of decennial precipitation for the state of Paraná. Irrigate. 2007; 12(1):38-53. (Portuguese)

37. De Souza EB, Moraes BC, Ferreira DBS, Meira Filho LG. Dynamical downscaling for railroad areas in Eastern Amazon and Southeastern Brazil: Current climate and near-future projections. Atmospheric and Climate Sciences. 2014; 4:155-163.

38. Marengo JA. Characteristics and spatio-temporal variability of the Amazon River Basin Water Budget. Climate Dynamics. 2005; 24(1):11-22.

39. Rosa DB, Sousa RR, Nascimento LA, Toledo LG, Topanotti DQ, Nascimento JÁ. The spatial distribution of rainfall in the Central-West portion of the State of Mato Grosso-Brazil. Electronic Magazine of the Association of Brazilian Geographers – Três Lagoas Section. 2007; 1(5):127-152. (Portuguese)

40. Salgueiro JHPB, Montenegro SMGL. Analysis of the spatial distribution of precipitation in the Pajeú river basin in Pernambuco according to geostatistical method. Fortaleza Technological Magazine. 2008; 29(2):174-185. (Portuguese)

41. Tucci CEM (Org.). Hydrology: science and application. 4th Ed., UFRGS Ed. – ABRH, Porto Alegre. 2012. (Portuguese)

42. Baú AL, Gomes BM, Queiroz MMF de, Opazo MAU, Sampaio SC. Spatial behavior of probable monthly rainfall in the western mesoregion of the State of Paraná. Irrigation, Botucatu. 2006; 11(2):150-168. (Portuguese)

43. Carvalho JRP de, Vieira SR. Validation of geostatistical models using Filliben test: application in agroclimatology. Embrapa Agricultural Informatics, Technical Communication, Campinas. 2004; 4 p. (Portuguese)

44. Mello JM de, Batista JLF, Júnior PJR, Oliveira MS de. Adjustment and selection of spatial semivariogram models aiming at volumetric estimation of Eucalyptus grandis. Scientia Forestalis. 2005; 69:25-37. (Portuguese)

45. Viola MR, Mello CR de, Pinto DBF, Mello JM de, Ávila LF. Spatial interpolation methods for mapping rainfall. Brazilian Journal of Agricultural and Environmental Engineering. 2010; 14(9):970-978. (Portuguese)

46. Carvalho JRP, Assad ED, Pinto HS. Geostatistical interpolators in the analysis of the spatial distribution of annual precipitation and its relationship with altitude. Brazilian Agricultural Research. 2012; 47(9):1235-1242. (Portuguese)

Sneha Babu R., & Uma G. (2023). Analyzing the Impact of Rainfall Patterns on Agriculture, Economy and Tourism in India: A Statistical Approach. International Journal of Environment and Climate Change, 13(11), 4626–4637. https://doi.org/10.9734/ijecc/2023/v13i113642

Gitima, G., & Mersha, M. (2020). The Impacts of El-Niño-Southern Oscillation (ENSO) on Agriculture and Coping Strategies in Rural Communities of Ethiopia: Systematic Review Article. Asian Journal of Geographical Research, 3(4), 56–69. https://doi.org/10.9734/ajgr/2020/v3i430117

Basso B, Fiorentino C, Cammarano D, Cafiero G, Dardanelli J. Analysis of rainfall distribution on spatial and temporal patterns of wheat yield in Mediterranean environment. European Journal of Agronomy. 2012 Aug 1;41:52-65.